IEEE Access
Multidisciplinary | Rapid Review | Open Access Journal

Received October 18, 2020, accepted October 28, 2020, date of publication November 3, 2020, date of current version November 17, 2020.

Digital Object Identifier 10.1109/ACCESS.2020.3035403

A New Denoising Method for Underwater Acoustic Signal

HONG YANG, LULU LI, AND GUOHUI LI
School of Electronics Engineering, Xi'an University of Posts and Telecommunications, Xi'an 710121, China
Corresponding authors: Hong Yang (uestcyhong@163.com) and Guohui Li (lghcd@163.com)

This work was supported by the National Natural Science Foundation of China under Grant 51709228.

ABSTRACT In recent years, the rapid development of marine science has put forward higher and higher requirements for the processing of ship-radiated noise signal. Ship-radiated noise is the noise signal generated by the vibration of various mechanical equipment or the movement of the hull and radiated into the sea when the ship is traveling. Ship-radiated noise signal contains a large number of time-varying, nonlinear and non-stationary components. The denoising processing of ship-radiated noise is the most critical part of underwater acoustic signal processing. In order to more effective reduce the noise of the ship-radiated noise signal, a new denoising method for underwater acoustic signal based on mutual information variational mode decomposition (MIVMD), multivariate multiscale dispersion entropy (mvMDE), and lift wavelet threshold (LWTD) and Savitzky Golay filter (S-G filter), named MIVMD-mvMDE-LWTD-SG, is proposed. Firstly, MIVMD is used to decompose the original signal into n sub-signals. Secondly, the mvMDE value of each sub-signal is calculated, and the n sub-signals are divided into high-frequency components and low-frequency components according to the threshold. Then, S-G filter and LWTD method are used to reduce the noise of low-frequency components and high-frequency components respectively. Finally, the low-frequency components and high-frequency components after the denoising processing are reconstructed to obtain the denoising signal. In order to verify the effectiveness of the proposed method, the proposed method is used to reduce the noise of chaotic signal under different signal-to-noise ratios (SNR), and compared with the EMD-mvMDE-LWTD and MIVMD-mvMDE-LWTD method. The results show that the proposed method can effective remove the noise in the chaotic signal, better distinguish the adjacent trajectories in the phase space, approximate the real chaotic attractor trajectory, and better retain the useful information in the chaotic signal. The proposed method is further applied to the actual ship-radiated noise signal, and the experimental analysis shows its effectiveness, which lays a solid foundation for further prediction and detection.

INDEX TERMS Mutual information variational mode decomposition, multivariate multiscale dispersion entropy, lift wavelet threshold, chaotic signal, denoising.

I. INTRODUCTION

With the rapid development of marine technology, the processing of underwater acoustic signal has become more and more important. Underwater target signal is affected by ship equipment and complex marine environment in the process of propagation, so that it contains a lot of useless noise signals and seriously affects the follow-up work. Therefore, using reliable method to remove noise is a hot issue in marine research. The traditional linear filtering noise reduction method can completely eliminate the noise in the periodic signal [1]. However, the ship-radiated noise is a typical non-Gaussian, non-stationary and nonlinear chaotic signal [2]–[4], so that the noise reduction effect of the linear filtering method is greatly reduced [5]. Therefore, some scholars are actively searching for more effective denoising methods.

In recent years, some scholars have proposed a variety of noise reduction methods for ship-radiated noise such as wavelet transform [6], [7], local projection [8], [9], singular spectrum analysis [10], independent component analysis [11], principal component analysis [12], compressed

The associate editor coordinating the review of this manuscript and approving it for publication was Yue Zhang.

sensing [13], and so on. Although the above methods can reduce the noise of ship-radiated noise to some extent, they all have their own limitations. For example, the basis function and the decomposition layers of wavelet transform cannot be selected adaptively, the neighborhood radius setting of local projection is difficult, and singular value decomposition is only effective when there are obvious noise platforms in the singular spectrum, etc. Aiming at nonlinear and non-stationary signal, Huang *et al.* proposed a new adaptive signal processing method, named empirical mode decomposition (EMD) [14]. Empirical mode decomposition can decompose the signal according to its own time-scale characteristics without setting the basis function in advance. EMD has been widely used in different fields as soon as it was proposed, and some improved algorithms such as ensemble empirical mode decomposition (EEMD) [15], complete ensemble empirical mode decomposition with adaptive noise (CEEMDAN) [16], masking signal empirical mode decomposition (MSEMD) [17], uniform phase empirical mode decomposition (UPEMD) [18], and so on, have been derived. EMD and its improved algorithm provides a new idea for noise reduction of ship-radiated noise, which is ''decompose the signal first and then reduce the noise''. Among them, typical methods are EMD and wavelet threshold method [19], noise adaptive EMD and correlation coefficient method [20], CEEMDAN, mutual information, permutation entropy (PE) and wavelet threshold method [21], UPEMD and amplitude-aware permutation entropy [22]. However, EMD and its improved algorithm belong to the empirical decomposition algorithm and lack a strict mathematical theoretical basis. Konstantin *et al.* proposed variational mode decomposition (VMD) in 2014 [23]. Compared with EMD and its improved algorithm, VMD is more reliable to decompose signals on the basis of strict mathematical theories, which are Wiener filtering, Hilbert transform, and signal analysis [24]. Moreover, VMD determines the center frequency and bandwidth of each component by iteratively searching and constructing a variational model, which shows good noise immunity and robustness. VMD is widely used in signal processing [25], [26], fault diagnosis [27], [28], wind speed prediction [29], [30] and other fields. But the most prominent shortcoming of VMD is that the decomposition number K value cannot be selected adaptively, and it needs to be preset manually [31], [32]. Mutual information (MI) is used to measure the dependence between two signals, and it is more effective than the correlation coefficient [33]. Aiming at the problem, this paper proposes mutual information variational mode decomposition (MIVMD), which determines the K value by judging the difference in mutual information values of between two adjacent sub-signal and the original signal.

Shannon entropy is a measure of the degree of system order. Shannon entropy has been widely used in different fields since it was proposed. Some scholars have successively proposed some improved algorithms of shannon entropy such as approximate entropy (ApEn) [34], sample entropy (SE) [35] and fuzzy entropy (FuzzyEn) [36], etc. Although the approximate entropy and its improved algorithm have strong anti-noise interference ability, the calculation speed is slow when the data length is large. Therefore, Bandt *et al.* proposed permutation entropy from different perspective based on the permutation mode of signal [37]. Although the calculation of permutation entropy is simple and efficient, the amplitude information of the signal is not considered. In response to this problem, Azami *et al.* proposed dispersion entropy (DE) in 2016 [38]. DE combines the advantages of permutation entropy and sample entropy. In 2017, Azami *et al.* coarsened DE and proposed multiscale dispersion entropy (MDE) [39]. MDE can measure the dispersion entropy of the signal at different time scales. In 2019, Azami *et al.* proposed the multivariate multiscale dispersion entropy(mvMDE) by combining the multivariate entropy with the coarse-grained process [40]. mvMDE realizes the measurement of multivariable signal complexity. Compared with existing method, mvMDE has fast calculation speed, strong stability and high recognition rate. Therefore, this article uses mvMDE value to classify sub-signals, and it is applied to the noise reduction of ship-radiated noise for the first time.

It is generally believed that the ship-radiated noise signal is located in the high-frequency band, and the real signal is located in the low-frequency band [41]. At present, denoising method of ship-radiated noise signal can be divided into two categories based on the idea of decomposing first and then noise reduction: (i) the signal is decomposed into n components, the high-frequency components are determined to be noise and directly removed. Then the low-frequency components are reconstructed [22], [41], [42]. (ii) it is determined that the high-frequency components contain useful information and its noise reduction is performed. Then the high-frequency components after noise reduction and the low-frequency components without noise reduction are reconstructed [43]–[45]. Our research found that both high-frequency components and low-frequency components have useful information and noise information, so there are problems in removing high-frequency components directly and reducing noise only in high-frequency components. Therefore, according to the characteristics of different sub-signals, we adopt different methods to reduce the noise of high-frequency and low-frequency components respectively. Reference [46] mentioned that the lifting wavelet threshold (LWTD) is used to reduce the noise of high-frequency signal, which can obtain a higher signal to noise ratio (SNR) and is more suitable for practical application. References [47], [48] pointed out that Savitzky Golay filter (S-G filter) is used to reduce the noise of low-frequency signal so that it can effectively retains the useful information of the low-frequency part. Therefore, in this paper, the lifting wavelet threshold is used to reduce the noise of high-frequency components, and the S-G filtering is used to reduce the noise of low-frequency components.

In order to reduce the noise of ship-radiated noise more effectively, this paper proposes a new denoising method for underwater acoustic signal based on MIVMD, mvMDE,

LWTD and S-G filter, named MIVMD-mvMDE-LWTD-SG. Firstly, aiming at the difficulty of presetting K value for VMD, a MIVMD method is proposed, and MIVMD is used to decompose the original signal into n sub-signals. Secondly, we use the mvMDE value of the sub-signal to divide the n sub-signals into high-frequency components and low-frequency components. Then, S-G filter and LWTD method are used to denoise the low-frequency components and high-frequency components, respectively. Finally, we reconstruct the low-frequency components and high-frequency components after the noise reduction to obtain the noise reduction signal.

The structure of this paper is as follows: Section II introduces the basic theory of VMD, MIVMD, mvMDE, LWTD and S-G filter. Section III introduces the proposed noise reduction method and evaluation index. Section IV is about the experiments for denoising of chaotic signal and ship-radiated noise as well as their result analysis. The discussions are displayed in Section V. The conclusions are summarized in Section VI.

II. BASIC THEORY

A. VARIATIONAL MODE DECOMPOSITION

Variational mode decomposition considers that the signal is superimposed by sub-signals with different frequencies dominate, and its purpose is to decompose the signal into sub-signals of different frequencies. Each sub-signal has its own center frequency and limited band width. Each sub-signal is defined as an AM/ FM signal as follows:

$$u_k(t) = A_k(t)\cos[\varphi_k(t)] \tag{1}$$

where $\varphi_k(t)$ is the phase of the signal, $A_k(t)$ is the instantaneous amplitude of the signal, $\omega_k(t)$ is the instantaneous frequency of the signal, and:

$$\omega_k(t) = \varphi_k'(t) = \frac{d\varphi_k(t)}{dt} \tag{2}$$

The main framework of variational mode decomposition is the variational problem, which minimizes the sum of the estimated bandwidth of each sub-signal [49]. The construction steps of the constrained variational model are as follows:

Step 1: Hilbert transform was applied to the original signal. We can obtain the corresponding analytic signal of each sub-signal, that is:

$$\left(\delta(t) + \frac{j}{\pi t}\right)^* u_k(t) \tag{3}$$

Step 2: After adding correction coefficients to the analytical signal corresponding to each sub-signal, the spectrum is transferred to the base band. The corresponding demodulated signal can be obtained:

$$\left[\left(\delta(t) + \frac{j}{\pi t}\right)^* u_k(t)\right] * e^{-j\omega_k t} \tag{4}$$

Step 3: The gradient square L^2 norm of the modulated signal is calculated to obtain the bandwidth of each sub-signal. The constructed constrained variational model is as follows:

$$\begin{cases} \min\limits_{\{u_k\}\{\omega_k\}} \left\{ \sum\limits_{k=1}^{K} \left\| \partial_t \left[\left(\delta(t) + \frac{j}{\pi t}\right)^* u_k(t) \right]^* e^{-j\omega_k t} \right\|_2^2 \right\} \\ s.t. \sum\limits_{k=1}^{K} u_k(t) = f(t) \end{cases} \tag{5}$$

where $u_k(t)$ represents the decomposed K sub-signals, $\omega_k(t)$ represents the center frequency of each sub-signal, δ (t) represents the unit pulse function, ∂_t represents the partial derivative of a function, * represents the convolution operation.

Step 4: The penalty factor α and lagrangian multiplier λ are introduced to transform the constrained variational problem into an unconstrained variational [50]. Thus the augmented lagrangian expression is obtained:

$$\begin{aligned} &L(\{u_k\}, \{\omega_k\}, \lambda) \\ &= \alpha \sum_{k=1}^{K} \left\| \partial_t \left[\left(\delta(t) + \frac{j}{\pi t}\right) u_k(t) \right] e^{-j\omega_k t} \right\|_2^2 \\ &\quad + \left\| f(t) - \sum_{k=1}^{K} u_k(t) \right\|_2^2 + \left\langle \lambda(t), f(t) - \sum_{k=1}^{K} u_k(t) \right\rangle \end{aligned} \tag{6}$$

This uncostrained problem is solved by the alternating direction method of multiplication operator, and all sub-signals of signal decomposition are finally obtained by iterative updating u_k^{n+1}, ω_k^{n+1}, λ_k^{n+1} [51].

$$\hat{u}_k^{n+1}(\omega) = \frac{\hat{f}(\omega) - \sum\limits_{i \neq k} \hat{u}_i(\omega) + \frac{\hat{\lambda}(\omega)}{2}}{1 + 2\alpha(\omega - \omega_k)^2} \tag{7}$$

$$\hat{\omega}_k^{n+1} = \frac{\int_0^\infty \omega \left|\hat{u}(\omega)\right|^2 d\omega}{\int_0^\infty \left|\hat{u}(\omega)\right|^2 d\omega} \tag{8}$$

$$\hat{\lambda}^{n+1}(\omega) = \hat{\lambda}^n(\omega) + \tau\left[\hat{f}(\omega) - \sum_k \hat{u}_k^{n+1}(\omega)\right] \tag{9}$$

B. MUTUAL INFORMATION VARIATIONAL MODE DECOMPOSITION

When VMD is used to decompose the signal, it is necessary to set the number of sub-signal K value in advance. The selection of K value directly determines the frequency resolution and has a greater impact on the decomposition effect. In order to avoid artificially preset inaccuracies, we need to adaptively guide the selection the number of decomposition.

The dependency between the original signal and the sub-signal obtained by VMD can be characterized by MI. MI is used to reflect the degree of correlation between two random variables and its ability of distinguish correlation is higher than the correlation coefficient method [52]. The mutual information of two discrete random variables is defined as:

$$I(X;Y) = \sum_{y \in Y} \sum_{x \in X} p(x,y) \log \frac{p(x,y)}{p(x)p(y)} \tag{10}$$

where $p(x, y)$ is the joint probability distribution function of two random variables, $p(x)$ and $p(y)$ is the marginal probability distribution function of X and Y respectively.

We gradually increase the K value decomposition signal, and it can be found that as the number of decompositions increases, the difference in mutual information values of between two adjacent sub-signal and the original signal shows a decreasing trend as a whole. When a threshold is reached, the signal is deemed to be sufficiently decomposed. Through a lot of experiments, it is found that the decomposition effect is best when the threshold is 0.1, so the threshold is set to 0.1. Therefore, in order to choose the best K value, we propose a method based on mutual information for selecting the number of decomposition, which is named MIVMD. The specific process is shown in FIGURE 1.

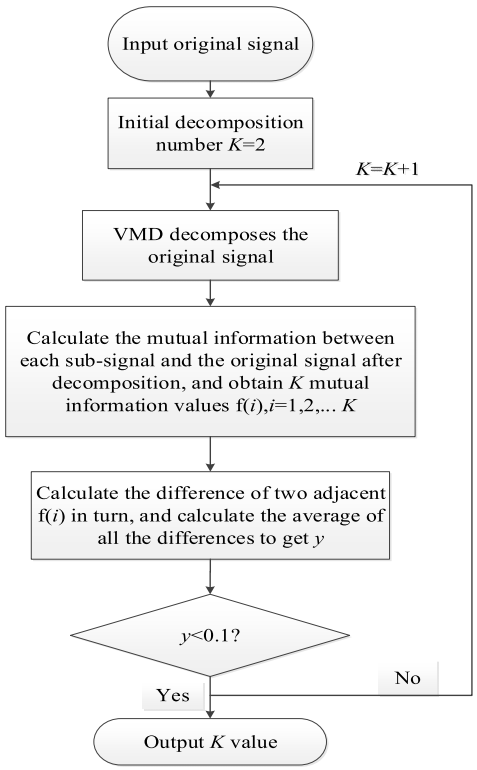

FIGURE 1. The flow chart of MIVMD.

C. MULTIVARIATE MULTISCALE DISPERSION ENTROPY

Compared with multiscale entropy, multivariate multiscale entropy can make multi-channel observation of the dynamic complexity of data [53]. In order to overcome the problem of mvMSE, Hamed Azami *et al.* proposed multivariate multiscale dispersion entropy (mvMDE) in 2019, which has the advantage such as fast calculation speed, good stability, and few storage elements [40]. The calculation process of mvMDE is as follows:

Step 1: Coarse-graining process of multivariate signals

Assume that a time series has p variables and its length is L. For each variable, the original signal is divided into non-overlapping segments of length τ. Then, the average value of each segment is calculated to derive the coarse-grained signal:

$$x_{k,i}^{(\tau)} = \frac{1}{\tau} \sum_{b=(i-1)\tau+1}^{i\tau} u_{k,b}, 1 \le i \le \left\lfloor \frac{L}{\tau} \right\rfloor = N, \quad 1 \le k \le p \tag{11}$$

where N represents the length of the coarse-grained signal.

Step 2: Multivariate dispersion entropy

(1) The multivariate signal $X = \left\{x_{k,i}\right\}_{k=1,2,\cdots,p}^{b=1,2,\cdots,N}$ is mapped into [1, 2, 3,..., c].

(2) In order to consider the space domain and time domain at the same time, a multivariate embedding vector is created based on the Takens embedding theorem $Z_m(j)$, $1 \le j \le N - (m-1)d$. For simplicity, we assume that $d_k = d, m_k = m$.

(3) All combinations of $\sum_{k=1}^{p} m_k$ elements take m once in $Z_m(j)$ and are called $\phi_q(j)(q = 1, \cdots, (\frac{mp}{m}))$. The number of combinations is equal to $\left(\frac{mp}{m}\right)$. Therefore, there is $(N-(M-1)d)(\frac{mp}{m})$ dispersion modes for all variables.

(4) For the latent dispersion mode $\pi_{v_0,\ldots v_{m-1}}$ corresponding to each c^m and $1 \le q \le \left(\frac{mp}{m}\right)$, the relative frequency is as follows:

$$p(\pi_{v_0 \cdots v_{m-1}}) = \frac{\#\left\{j \,|j \le N-(m-1)d, \phi_q(j)\ hastype \pi_{v_0,\cdots v_{m-1}}\right\}}{(N-(m-1)d)\left(\frac{mp}{m}\right)} \tag{12}$$

(5) According to the definition of Shannon entropy, mvDE can be expressed as:

$$mvDE(X, m, c, d) = -\sum_{\pi=1}^{c^m} p(\pi_{v_0 \cdots v_{m-1}}) \cdot \ln(p(\pi_{v_0 \cdots v_{m-1}})) \tag{13}$$

Both mvMDE, mvMSE and mvMFE have the ability to detect the dynamic characteristics of multivariable signal. In order to verify the performance of mvMDE, this paper quantitatively analyzes related indexes of mvMDE, mvMSE and mvMFE. We randomly generate a set of noise signals such as a Gaussian white noise, a Rayleigh distribution noise, and a K distribution noise, calculate the mvMDE, mvMSE and mvMFE values of 11 scales of noise, and count their computing time (CT). CT is an indicator of the running time of the algorithm. The mvMDE, mvMSE and mvMFE values of noise are shown in FIGURE 2, and the running times of the three entropies are given in TABLE 1.

FIGURE 2 shows that mvMDE and mvMFE have a more stable profile and good stability than mvMSE. But mvMDE can better identify noise signal of different scales than mvMFE. TABLE 1 shows that mvMDE runs faster and more efficient. Therefore, mvMDE is more suitable for analyzing the complexity of nonlinear and non-stationary signal.

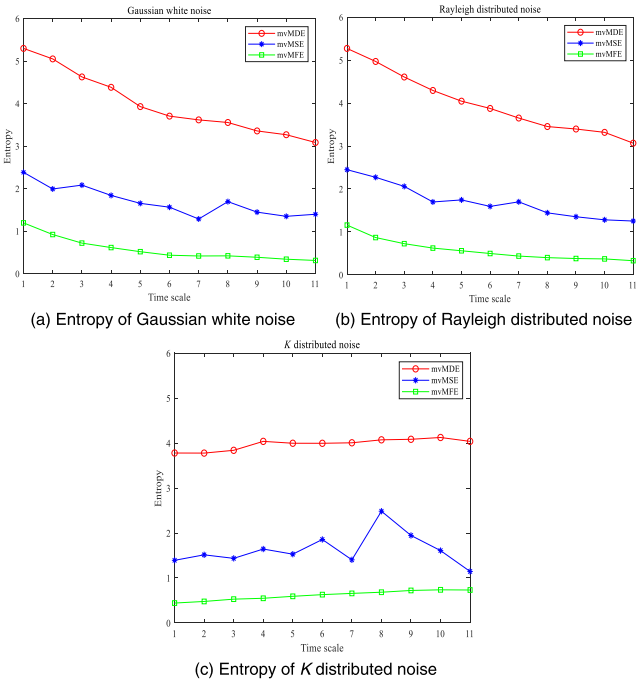

(a) Entropy of Gaussian white noise (b) Entropy of Rayleigh distributed noise

(c) Entropy of *K* distributed noise

FIGURE 2. Entropy of different noises.

TABLE 1. Running time of three kinds of entropy.

CT/s	mvMDE	mvMSE	mvMFE
Gaussian white noise	0.0561	0.0823	0.1721
Rayleigh distributed noise	0.0658	0.0845	0.1765
K distributed noise	0.0731	0.0852	0.1921

D. SAVITZKY-GOLAY FILTER

Savitzky-Golay filter is a polynomial smoothing algorithm based on the principle of least squares proposed by Savitzky and Golay, which is widely applied to the filtering of non-stationary signal under non-Gaussian background noise [54], [55]. While filtering and smoothing, it can more effectively retain signal change information.

Firstly, a total of $2M+1$ data before and after the current moment is filtered, and we use Equation (14) for fitting [56]:

$$p(n) = \sum_{k=0}^{N} a_k \cdot n^k \tag{14}$$

The residual after fitting is:

$$\varepsilon_N = \sum_{n=-M}^{M} (p(n) - x(n))^2 = \sum_{n=-M}^{M} (\sum_{k=0}^{N} a_k \cdot n^k - x(n))^2 \tag{15}$$

Perform a weighted average operation on $2M+1$ data that can solve the constant term of the fitted polynomial:

$$y(n) = \sum_{m=-M}^{M} h(m) \cdot x(n-m) = \sum_{m=n-M}^{n+M} h(n-m) \cdot x(m) \tag{16}$$

The partial derivative of the residual formula can be obtained:

$$\begin{aligned} \frac{\partial \varepsilon_N}{\partial a_i} &= \sum_{n=-M}^{M} 2n^i (p(n) - x(n))^2 \\ &= \sum_{n=-M}^{M} 2n^i (\sum_{k=0}^{N} a_k \cdot n^k - x(n))^2 = 0 \end{aligned} \tag{17}$$

Simplification can get:

$$\sum_{k=0}^{N} (\sum_{n=-M}^{M} n^{i+k}) \cdot a^k = \sum_{n=-M}^{M} n^i \cdot x(n), \quad i = 0, 1, \cdots, N \tag{18}$$

Let $A = \{a_{ni}\} = \left\{n^i\right\}, -M \le n \le M, 0 \le i \le N, B = A^{\mathrm{T}} \cdot A$, then

$$b_{ik} = \sum_{n=-M}^{M} a_{in} a_{nk} = \sum_{n=-M}^{M} n^{i+k} = b_{ki} \tag{19}$$

Therefore,

$$Ba = A^{\mathrm{T}} \cdot Aa = A^{\mathrm{T}} x, a = \left(A^{\mathrm{T}} \cdot A\right)^{-1} \cdot A^{\mathrm{T}} x = Hx \tag{20}$$

where H is the required coefficient.

E. LIFT WAVELET THRESHOLD TO REDUCE NOISE

Compared with the traditional wavelet transform, it relies very much on the Fourier transform. The lifting wavelet transforms in the time domain and does not depend on the Fourier transform. At the same time, it can realize all the first-generation wavelet transform. The lifting wavelet not only inherits the characteristics of the first-generation wavelet multi-resolution, but also has simple calculation and less memory, which overcomes the shortcoming of the first-generation wavelet transform [57], [58]. The general lifting wavelet process can be divided into three steps:

Step 1: Split. The signal $x(n)$ is splitted into two non-overlapping subsets according to the odd-even sequence, which is divided into even sequence and odd sequence:

$$\begin{aligned} x_o(n) &= x(2k+1), \quad k = 1, 2, \cdots \\ x_e(n) &= x(2k), \quad k = 1, 2, \cdots \end{aligned} \tag{21}$$

Step 2: Predict. The signal has local correlation, and the value of the odd sequence can be predicted by the value of the adjacent even sequence [59]. The predicted error is the transform coefficient of wavelet transform:

$$d(n) = x_o(n) - P(x_e(n)) \tag{22}$$

Step 3: Update. Introduce an update operator U to modify $d(n)$, which $a(n)$ represents the scale factor of wavelet decomposition:

$$a(n) = x_e(n) + U\left(d\left(n\right)\right) \tag{23}$$

The lifting wavelet is realized by $x_e(n)$ iterations. The reconstruction process of the lifting wavelet is the inverse process of the decomposition process [60]:

$$\begin{aligned} x_e(n) &= a(n) - U(d(n)) \\ x_o(n) &= d(n) + P(x_e(n)) \\ x(n) &= Merge(x_e(n), x_o(n)) \end{aligned} \tag{24}$$

where $Merge(\cdot)$ represents the merger.

The selection of the threshold function is very important for lifting the wavelet threshold to reduce noise [61]. The commonly used lifting wavelet threshold methods include hard threshold method and soft threshold method. The soft threshold method is proposed to overcome the ''one size fits all'' drawback of the hard threshold method. The hard threshold method is simple and has poor continuity. Compared with the hard threshold method, the soft threshold method has a smoother noise reduction signal.

III. THE PROPOSED NOISE REDUCTION METHOD AND EVALUATION INDEX

A. THE PROPOSED NOISE REDUCTION METHOD

The basic principles of MIVMD, mvMDE, S-G filter and LWTD threshold are introduced in Section II. As a widely used data denoising method, S-G filter has achieved good result in various application [62]. As a new and improved dispersion entropy, multivariate multiscale dispersion entropy has few practical application. Therefore, a new noise reduction method for underwater acoustic signal based on MIVMD, mvMDE, LWTD and S-G filter, called MIVMD-mvMDE-LWTD-SG, is proposed. Specific steps are as follows:

Step 1: Use MIVMD to decompose ship-radiated noise into n IMFs.

Step 2: Calculate the mvMDE of each IMF. Set the threshold value t in this paper. Consider IMF greater than t as high-frequency components, and IMF smaller than t as low-frequency components.

Step 3: Use the S-G filtering method for low-frequency components to reduce noise, and use the lifting wavelet soft threshold method for high-frequency components to reduce noise.

Step 4: Reconstruct the low-frequency and high-frequency components after the noise reduction process to obtain the final noise reduction signal.

B. EVALUATION INDEX

In order to quantitatively analyze the effect of noise reduction, this paper uses some evaluation indicators to quantify the signal before and after noise reduction.

1) SIGNAL TO NOISE RATIO

Signal to noise ratio (SNR) represents the ratio of signal to noise power. The greater the SNR of the signal, the less the noise content; the smaller the SNR of the signal, the greater the noise content. The SNR is defined as:

$$SNR = 10\log_{10}\left(\frac{\|x(n)\|^2}{\left\|\hat{x}(n) - x(n)\right\|^2}\right) \tag{25}$$

where $x(n)$ represents a pure signal and $\hat{x}(n)$ represents a noisy signal.

2) ROOT MEAN SQUARE ERROR

Root mean square error (RMSE) represents the difference between the noise reduced signal and the pure signal [63]. The smaller the RMSE, the better the noise reduction effect; the larger the RMSE, the worse the noise reduction effect. The root mean square error is defined as:

$$RMSE = \sqrt{\frac{\left\|\hat{x}(n) - x(n)\right\|^2}{N}} \tag{26}$$

where N is the length of the signal, $x(n)$ represents a pure signal, and $\hat{x}(n)$ represents a noisy signal.

3) CORRELATION DIMENSION

Fractal dimension is an index to measure the complexity and irregularity of attractor in dynamic process. Correlation dimension, as a kind of fractal dimension, has been widely used in mechanical fault diagnosis [64], seismic exploration [65] and other fields. The calculation of the correlation dimension is mainly realized by the G-P algorithm [66]. Firstly, embed a new dimension m in a time series, and perform phase space reconstruction to get:

$$X(n) = \begin{bmatrix} X_1 \\ X_2 \\ \vdots \\ X_k \end{bmatrix} = \begin{bmatrix} x_1 & x_2 & \cdots & x_m \\ x_2 & x_3 & \cdots & x_{m+1} \\ \vdots & \vdots & \vdots & \vdots \\ x_{n-m+1} & x_{n-m+2} & \cdots & x_n \end{bmatrix} \tag{27}$$

Choose an appropriate distance r and calculate the logarithm of the points whose distance is less than r:

$$C\left(r\right) = \frac{1}{N^2}\sum_{j=1}^{N}\sum_{i=1}^{N}\theta(r - \left|X_i - X_j\right|) \tag{28}$$

$$\theta(x) = \begin{cases} 0, & x < 0 \\ 1, & x \geq 0 \end{cases} \tag{29}$$

Finally, use the least square method to solve the correlation dimension:

$$D = \lim_{r\to 0}\frac{\ln(C(r))}{\ln(r)} \tag{30}$$

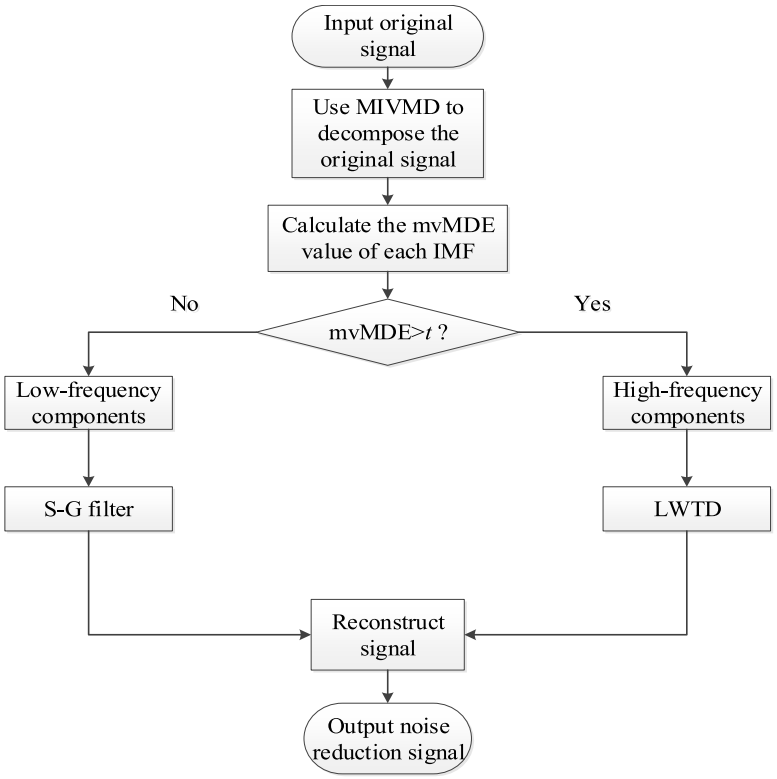

FIGURE 3. Flow chart of the proposed noise reduction method.

TABLE 2. Noise reduction effect of noisy signal.

Noisy Signal	EMD-mvMDE-LWTD		MIVMD-mvMDE-LWTD		MIVMD-mvMDE-LWTD-SG	
	SNR	RMSE	SNR	RMSE	SNR	RMSE
-5db	1.1807	8.1221	5.3702	5.0141	5.4122	4.9899
0db	7.7075	3.8311	9.2185	3.2194	9.3500	3.1710
5db	11.5258	2.4684	11.9278	2.3567	13.9975	1.8571
10db	15.7092	1.5249	15.4204	1.5764	16.6460	1.3690
15db	18.1968	1.1452	19.8008	0.9521	20.5159	0.8768

4) MAXIMUM LYAPUNOV EXPONENT

The Lyapunov exponent is an important index to measure the complexity of a dynamic system [67]. Lyapunov exponent refers to the average change rate of two orbits close to each other in the phase space as time goes by, which are separated or aggregated exponentially. In practical application, maximum Lyapunov exponent is of great significance, and the calculation formula is:

$$\lambda_1 = \frac{1}{t_m - t_0} \sum_{k=1}^{M} \ln \frac{D(t_k)}{D(t_{k-1})} \tag{31}$$

where $D(t_k)$ represents the distance between the two closest points at t_k time, M represents the total number of iteration steps. When the maximum Lyapunov exponent is positive, it indicates that the motion state of the system is chaotic. When the maximum Lyapunov exponent is zero, it indicates that the system is in a critically stable state. When the maximum Lyapunov exponent is negative, it indicates that the system is in a stable state.

IV. EXPERIMENTAL SIMULATION

A. NOISE REDUCTION OF CHAOTIC SIGNAL

In order to verify the effectiveness and feasibility of the proposed method, this paper uses the Chen system for experimental verification, which is expressed as follows:

$$\begin{aligned} \dot{x} &= a(y - x) \\ \dot{y} &= (c - a)x - xz + cy \\ \dot{z} &= xy - bz \end{aligned} \tag{32}$$

where $a = 35$, $b = 3$, $c = 28$, step size $h = 0.01$, variable initial value $x(0) = -1$, $y(0) = 0$, $z(0) = 1$.In this paper, 2048 points of the y variable are selected as pure signals, and Gaussian white noise of -5dB, 0dB, 5dB, 10dB and 15dB are added, respectively. This proposed method is compared with EMD-mvMDE-LWTD and MIVMD-mvMDE-LWTD by the

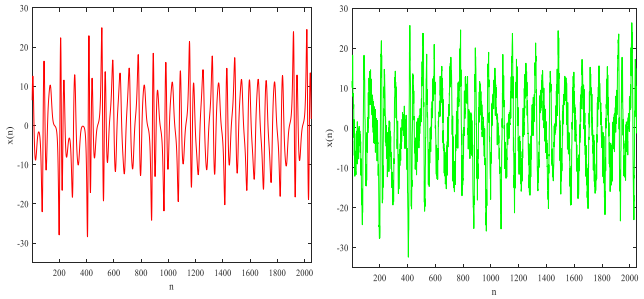

FIGURE 4. Time domain diagram of pure signal and noisy signal.

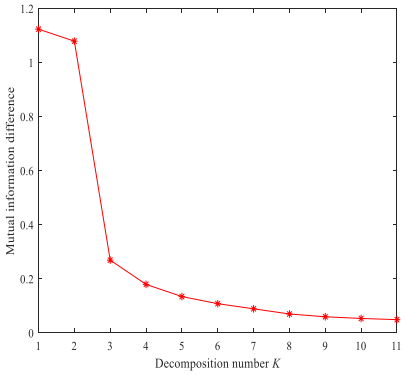

FIGURE 5. Mutual information difference trend graph.

same signal. Among them, EMD-mvMDE-LWTD uses EMD to decompose the signal into n sub-signals, and calculates mvMDE value of each sub-signal, then divides signal into high-frequency components and low-frequency components according to their mvMDE value. Then the method performs LWTD processing on high-frequency components, and reconstructs the processed conponents and low-frequency components to obtain the denoised signal. The flow of MIVMD-mvMDE-LWTD and EMD-mvMDE-LWTD methods are similar. The noise reduction effect of Chen noisy signal is shown in TABLE 2

In order to understand the detail of noise reduction in depth, this paper conducts a noise reduction study on the signal with 10dB noise. The time-domain waveform diagrams of the pure Chen signal and the noisy Chen signal are shown in FIGURE 4. Firstly, MIVMD is used to decompose the noisy Chen signal.

Before using MIVMD to decompose the noisy signal, the decomposition number K value should be determined. The trend of mutual information difference is shown in FIGURE 5.

It can be seen from FIGURE 5 that as the K value increases, the trend of the difference in mutual information values between two adjacent sub-signal and the original signal gradually decreases. When $K = 7$, the difference is 0.0894, which is less than the threshold, and the signal is fully decomposed. Therefore, the K value is set to 7. In this paper, we uniformly set the penalty factor of variational modal decomposition to the default value of 2000 [68]. The MIVMD decomposition results of the noisy signal are shown in FIGURE 6.

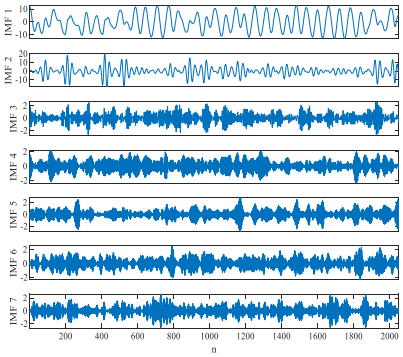

FIGURE 6. MIVMD decomposition.

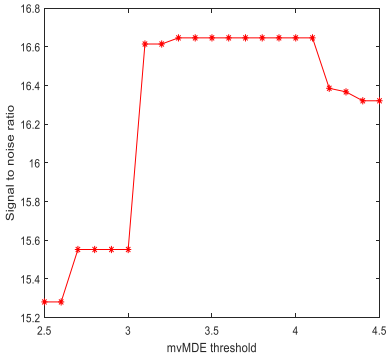

FIGURE 7. The SNR of the denoising signal under different thresholds.

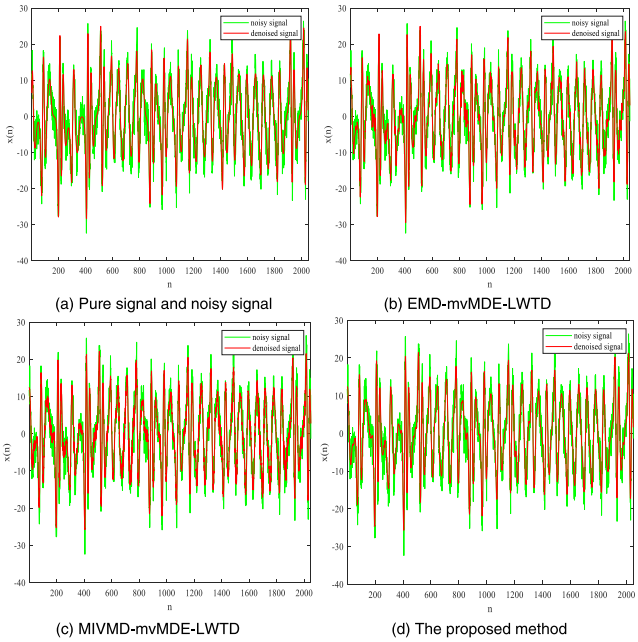

FIGURE 8. Waveform comparison before and after noise reduction.

Entropy is used to distinguish high and low frequency components. Under the premise of ensuring the noise reduction effect, we want the amount of computation to be as small as possible. TABLE 3 shows that mvMDE has the fastest operation time under scale 1. Therefore, we performed the entropy calculation at scale 1. The noisy signal is decomposed into 7 IMFs, and the mvMDE value of each IMF

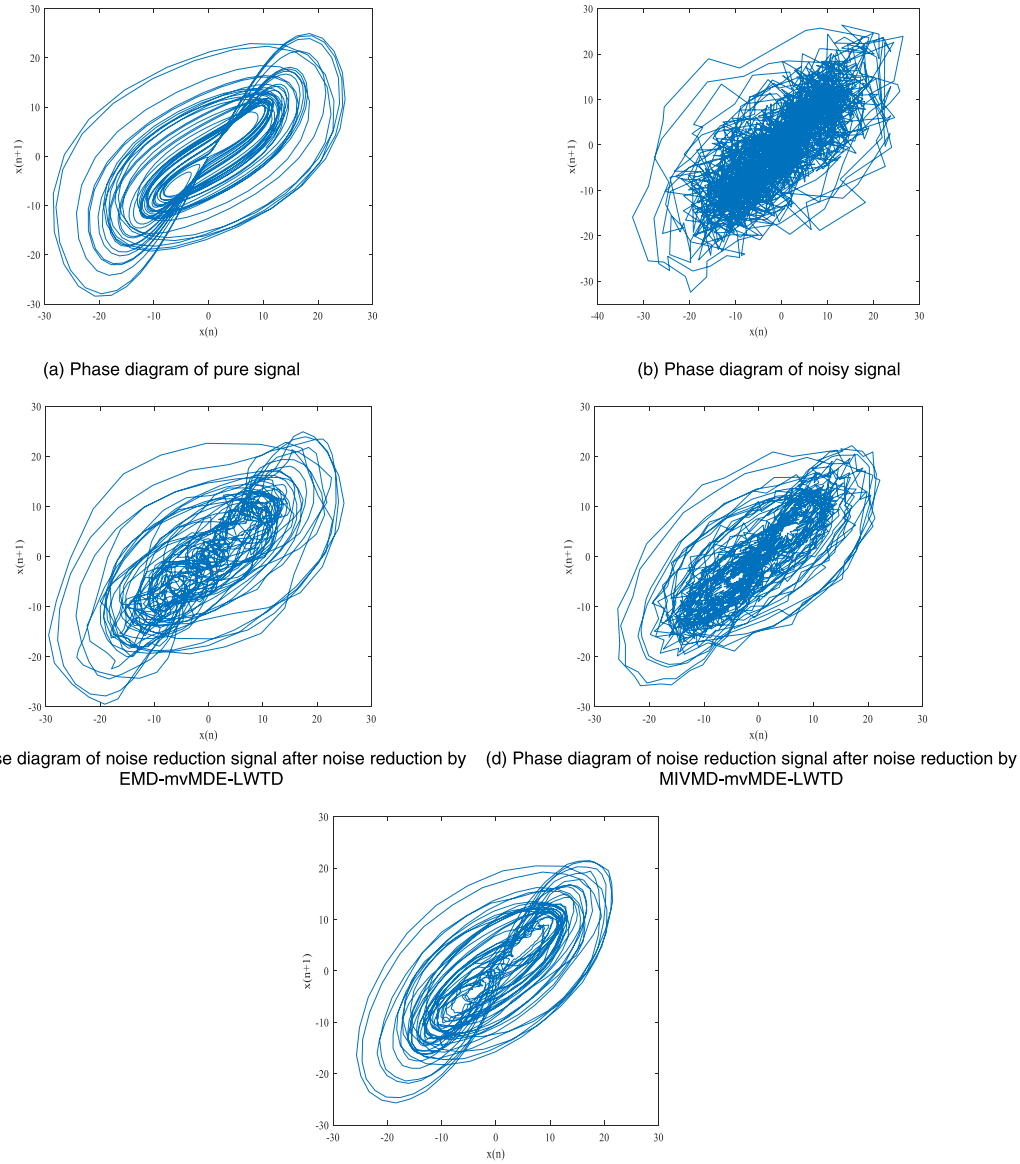

(a) Phase diagram of pure signal

(b) Phase diagram of noisy signal

(c) Phase diagram of noise reduction signal after noise reduction by EMD-mvMDE-LWTD

(d) Phase diagram of noise reduction signal after noise reduction by MIVMD-mvMDE-LWTD

(e) Phase diagram of noise reduction signal after noise reduction by the proposed method

FIGURE 9. Attractor phase diagram of noise reduction signal.

is calculated respectively. The entropy value is shown in TABLE 4. In order to get a suitable threshold, the threshold is set between 2.5 and 4.5, and the SNR of the method is calculated under different threshold values. The SNR diagram of noise reduction signals with different thresholds is shown in FIGURE 7.

FIGURE 7 shows that with the continuous increase of the threshold, the SNR after noise reduction first increases and then decreases. The SNR reaches the maximum value in the range of 3.3 to 4.1, and the SNR begins to drop when the threshold exceeds 4.1. In this experiment, IMF1, IMF2 and IMF7 are denoised by S-G filtering and IMF3∼IMF6 are denoised by lifting wavelet threshold to achieve the best denoising effect. After many experiments, this paper sets the threshold to 3.9.

TABLE 3. Under different scales, running time to calculate mvMDE for each IMF.

scale / CT/s / IMF	scale 1	scale 2	scale 3	scale 4
IMF1	0.0167	0.0773	0.0660	0.0551
IMF2	0.0203	0.0532	0.0620	0.0564
IMF3	0.0168	0.0530	0.0322	0.0464
IMF4	0.0160	0.0367	0.0568	0.0966
IMF5	0.0118	0.0456	0.0527	0.0610
IMF6	0.0107	0.0324	0.0695	0.0706
IMF7	0.0098	0.0209	0.0288	0.0601

In order to show the effect of noise reduction intuitively, the waveform comparison diagram before and after noise reduction using EMD-mvMDE-LWTD, MIVMD-mvMDE-LWTD and the proposed method are given.

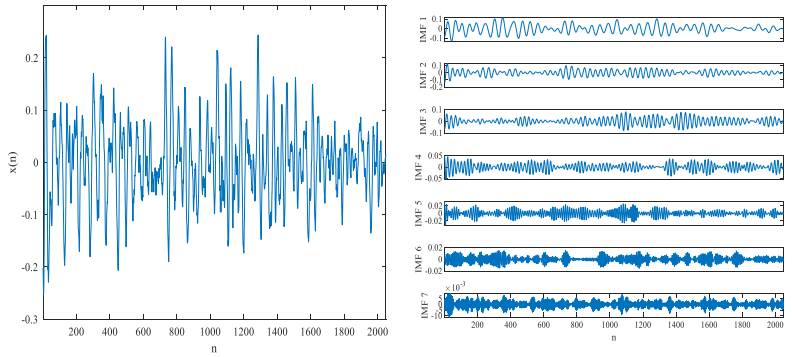

(a) The time domain waveform of Ship1 and MIVMD result

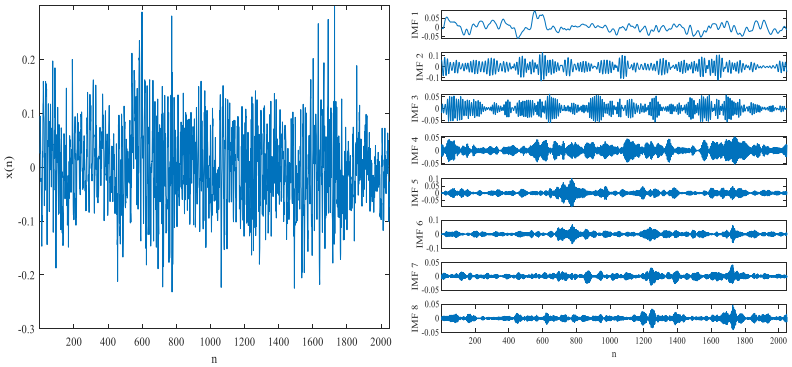

(b) The time domain waveform of Ship2 and MIVMD result

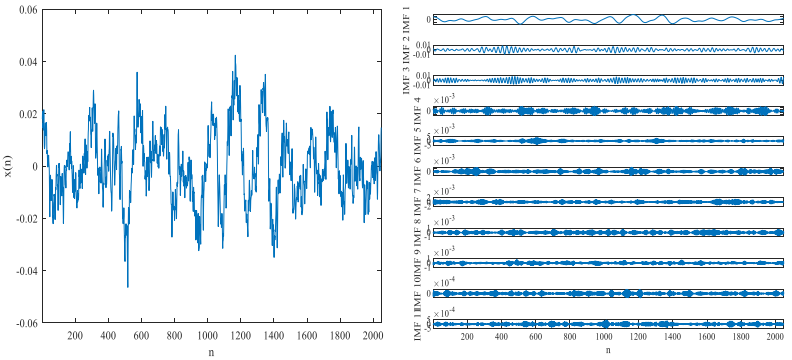

(c)The time domain waveform of Ship3 and MIVMD result

FIGURE 10. Time domain waveform diagram and decomposition result.

TABLE 4. The mvMDE value of each IMF.

IMF1	IMF2	IMF3	IMF4	IMF5	IMF6	IMF7
2.6898	3.0882	4.1791	4.3409	4.2408	4.2781	3.2550

The waveform comparison chart before and after noise reduction is shown in FIGURE 8.

It can be seen from the time domain waveform of the three noise reduction methods that, compared with EMD-mvMDE-LWTD and MIVMD-mvMDE-LWTD, the signal residual noise after using the proposed method to denoise is less, more smoother, and most similar to the pure signal. The motion characteristics of the chaotic signal can be expressed by the phase diagram method. In order to more intuitively reflect the noise reduction effect of different methods, the phase diagram of the attractor before and after noise reduction is further studied. The attractor phase diagram of the noise reduction signal is shown in FIGURE 9.

It can be seen from FIGURE 9 that although the phase diagram after noise reduction of using EMD-mvMDE-LWTD and MIVMD-mvMDE-LWTD methods has a certain improvement compared with the phase diagram before noise reduction, the trajectory of the phase diagram is severely twisted and too tortuous. The trajectory of the phase diagram after noise reduction by the proposed method in this paper is smoother, the geometric structure is more regular, and the phase diagram of the pure signal is closer. In addition, the mvMDE and the maximum Lyapunov exponent before and after noise reduction are also given to further analyze the signal characteristics quantitatively.

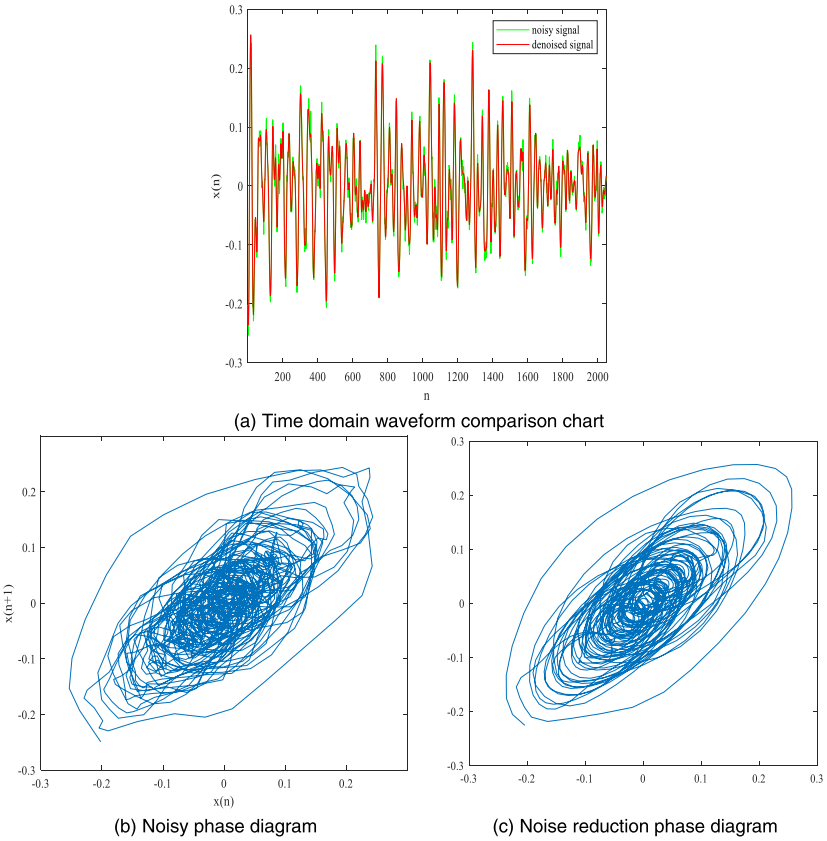

(a) Time domain waveform comparison chart

(b) Noisy phase diagram

(c) Noise reduction phase diagram

FIGURE 11. The time domain waveform and phase diagram of attractor before and after denoising for Ship1.

TABLE 5. Comparison of parameters before and after noise reduction.

Characteristic parameter	mvMDE	Maximum Lyapunov exponent
Noisy Chen signal	3.9586	0.5871
EMD-mvMDE-LWTD	3.0044	0.1831
MIVMD-mvMDE-LWTD	3.2657	0.1965
The proposed method	2.8857	0.1055

From the data in TABLE 5, it can be seen that compared with EMD-mvMDE-LWTD and MIVMD-mvMDE-LWTD methods, the improvement effect of this proposed method is the most obvious. The above experiments show that the proposed method has a good effect in noise reduction of chaotic signal.

B. NOISE REDUCTION OF SHIP-RADIATED NOISE

In order to verify the practicability of the proposed method in this paper, the noise reduction method is applied to the real ship-radiated noise. Three different types of noise signals are selected from the shipsear database (http://atlanttic.uvigo.es/underwaternoise/), named passenger ships, ocean liners and motor boats respectively [69]. The three kinds of signals are normalized and sampled separately, and 2048 points are sampled for each type of signal, and they are named Ship1, Ship2 and Ship3. The time-domain waveforms of three kinds of noise signals and the decomposition results of MIVMD are shown in FIGURE 10.

In order to intuitively reflect the detailed changes and dynamic characteristics of the ship-radiated noise signal before and after noise reduction, the time-domain waveform diagrams and attractor phase diagrams of three kinds of noise signals before and after noise reduction are studied, as shown in FIGURE 11, FIGURE 12 and FIGURE 13.

In addition, this paper also quantitatively analyzes the noise reduction effect of ship-radiated noise signal. The correlation dimension and maximum Lyapunov exponent of three kinds of signals before and after noise reduction are calculated respectively. The smaller the value of two parameters, the less the noise content of the signal and the better the noise reduction effect. The parameters of ship-radiated noise before and after noise reduction are shown in TABLE 6.

From the time-domain waveform comparison diagrams in FIGURE 11, FIGURE 12 and FIGURE 13, it can be seen that after using this proposed method to reduce the noise of three kinds of ship-radiated noise signals, the noise in the background is better removed and the change trend of waveform is clearer. From the phase diagrams before and after noise reduction, it can be seen that the phase diagram has changed from a messy, rough trajectory to a more regular, smoother trajectory. These phenomena show that this proposed method can better distinguish the adjacent trajectories in the phase

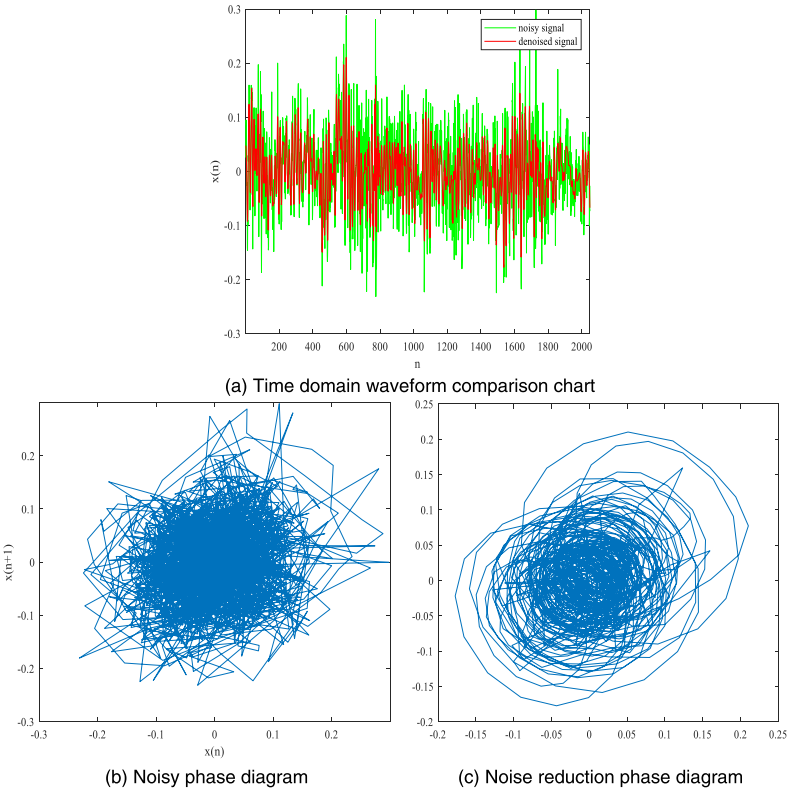

(a) Time domain waveform comparison chart

(b) Noisy phase diagram

(c) Noise reduction phase diagram

FIGURE 12. **The time domain waveform and phase diagram of attractor before and after denoising for Ship2.**

TABLE 6. **Comparison of parameters before and after noise reduction.**

Ship-radiated noise	Status	Correlation dimension	Maximum Lyapunov exponent
Ship1	Before denoising	1.7709	0.1026
	After denoising	1.7616	0.0897
Ship2	Before denoising	1.7721	1.1099
	After denoising	1.7428	0.3838
Ship3	Before denoising	1.8229	1.0200
	After denoising	1.7889	0.3136

space, approximate the real chaotic attractor trajectory, and effectively retain the real characteristics of chaotic dynamics. It can be seen from TABLE 6 that the parameter values of the three noise signals after noise reduction are all smaller than those before noise reduction. The above experiments show that the noise reduction method proposed in this paper can be applied to the treatment of real ship-radiated noise.

V. DISCUSSIONS

VMD is different from the traditional mode decomposition method. With its non-recursive decomposition method and strong analytical capability, it can effectively avoid the phenomenon of mode mixing. However, VMD needs to set the number of decomposition in advance before the signal decomposition. The proposed method in this paper selects the number of decomposition based on mutual information, which solves this problem and improves the self-adaptability of VMD. This will lay a certain foundation for its application.

As a new improved algorithm of MDE, mvMDE, proposed in 2019, has better stability, higher recognition rate and faster calculation efficiency than mvMSE and mvMFE in terms of measuring the complexity of time series. We applied it to the noise reduction of underwater acoustic signal for the first time, and got better results. In view of the advantages of mvMDE, it will have a broad application prospect in the fields of feature extraction, fault detection and signal prediction.

Noise in the actual underwater environment is usually generated by ship, marine equipment, marine life, submarine earthquake, marine industrial activity, surface wave, undersea exploration, and thermal noise, etc. Different types of noise components have different frequency ranges. The noise generated by ship, submarine earthquake, marine industrial activity, etc., are low-frequency signals. This indicates that the low-frequency components of ship-radiated noise signal decomposed are noisy. In addition, TABLE 6 and FIGURE 11, FIGURE 12, FIGURE 13 in this paper also verify this conclusion. Some data in TABLE 6 are not significantly improved by using the proposed method in this paper,

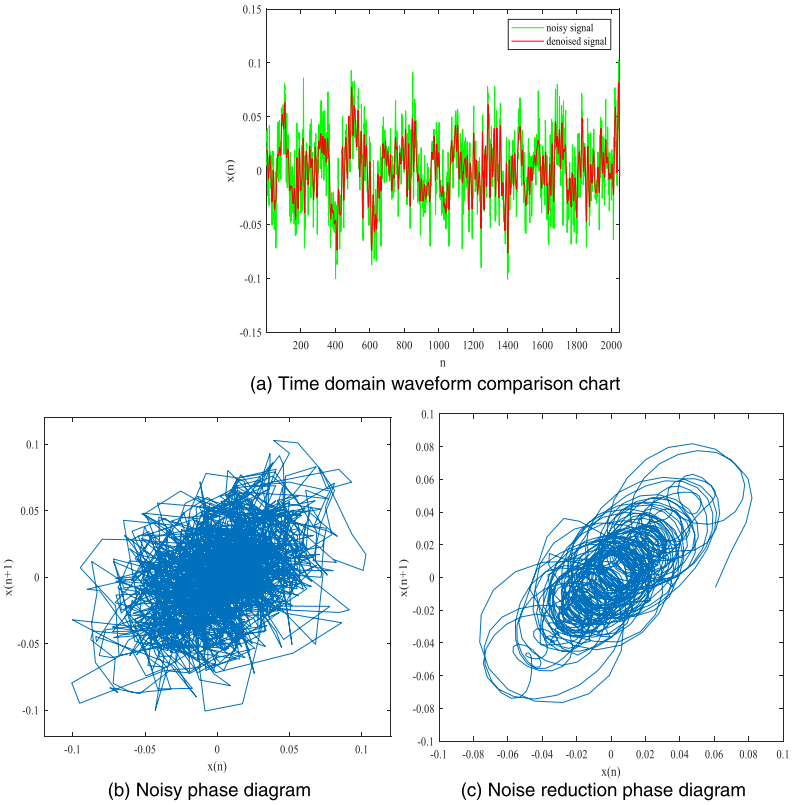

(a) Time domain waveform comparison chart

(b) Noisy phase diagram

(c) Noise reduction phase diagram

FIGURE 13. The time domain waveform and phase diagram of attractor before and after denoising for Ship3.

which indicates that there is a small amount of weak noise in the low-frequency components. Therefore, the low-frequency signal contains a small amount of weak noise. This provides a new idea and method for noise reduction of underwater acoustic signal.

VI. CONCLUSION

A new denoising method for underwater acoustic signal based on MIVMD, mvMDE, LWTD and S-G filter is proposed. The main conclusions of this article are as follows:

(1) Aiming at the shortcoming that VMD needs to set the decomposition number in advance before the decomposition of signals, this paper proposes a method to select the decomposition number based on mutual information, which improves the self-adaptability of VMD.

(2) As a new improved algorithm of MDE, mvMDE measures the complexity of time series. Compared with mvMSE and mvMFE, mvMDE has better stability, higher recognition rate and faster calculation efficiency. It is first applied to noise reduction of underwater acoustic signal and has great development potential in nonlinear signal processing.

(3) According to references [22], [41], [42] that the low-frequency components does not contain noise, our research found that the low-frequency components contains weak noise after the signal is decomposed, and more noise can be removed by denoising both the high-frequency components and low-frequency components.

(4) The proposed method is applied to chaotic signal. Compared with EMD-mvMDE-LWTD and MIVMD-mvMDE-LWTD, the proposed method has higher SNR and lower RMSE.

(5) The proposed method is applied to three real underwater acoustic signals. The experimental results show that the proposed method can obtain a more regular and smooth attractor phase diagram and remove more noise components. This will lay a solid foundation for the subsequent processing of ship-radiated noise signals such as prediction, detection, extraction and classification, and so on.

REFERENCES

[1] J. W. Yin, W. X. Luo, L. Li, X. Han, L. X. Guo, and J. F. Wang, "Enhancement of underwater acoustic signal based on denoising automatic-encoder," *J. Commun.*, vol. 40, no. 10, pp. 119–126, 2019.

[2] Y. Li, Y. Li, X. Chen, and J. Yu, "Denoising and feature extraction algorithms using NPE combined with VMD and their applications in ship-radiated noise," *Symmetry*, vol. 9, no. 11, p. 256, Nov. 2017.

[3] Z. Li, Y. Li, and K. Zhang, "A feature extraction method of ship-radiated noise based on fluctuation-based dispersion entropy and intrinsic time-scale decomposition," *Entropy*, vol. 21, no. 7, p. 693, Jul. 2019.

[4] Z. Chen, Y. Li, H. Liang, and J. Yu, "Hierarchical cosine similarity entropy for feature extraction of ship-radiated noise," *Entropy*, vol. 20, no. 6, p. 425, Jun. 2018.

[5] G. J. Tang, X. L. Yan, and X. L. Wang, "Chaotic signal denoising based on adaptive smoothing multiscale morphological filtering," *Complexity*, vol. 2020, Feb. 2020, Art. no. 7242943.

[6] L. L. Zhao and X. W. Dai, "De-noising of underwater acoustic weak signals based on compressed sensing technique," *Adv. Mater. Res.*, vols. 989–994, pp. 3718–3721, Jul. 2014.

[7] M. M. Khan, R. H. Ashique, B. N. Liya, M. M. Sajjad, M. A. Rahman, and M. T. H. Amin, "New wavelet thresholding algorithm in dropping ambient noise from underwater acoustic signals," *J. Electromagn. Anal. Appl.*, vol. 7, no. 3, pp. 53–60, 2015.

[8] H. M. Zheng, Y. A. Li, and L. Chen, "Noise reduction of ship signals based on the local projective algorithm," *J. Northwestern Polytech. Univ.*, vol. 29, no. 4, pp. 569–574, 2011.

[9] L. Cui, Y. A. Li, R. C. Liu, and G. H. Li, "Parameters determination of local projective algorithm and its application," *Audio Eng.*, vol. 35, no. 3, pp. 64–68, 2011.

[10] Y. A. Li, H. C. Wang, and J. Chen, "Research of noise reduction of underwater acoustic signals based on singular spectrum analysis," *Syst. Eng. Electron.*, vol. 29, no. 4, pp. 524–527, 2007.

[11] K. Wei and Y. Bin, "De-noising of underwater acoustic signals based on ICA feature extraction," in *Proc. 10th Iberoamerican Congr. Pattern Recognit.*, vol. 3773, 2005, pp. 917–924.

[12] Y. W. Wu, C. X. Xing, L. L. Yue, and X. J. Wan, "Noise reduction method of low frequency underwater acoustic signal based on robust principal component analysis," *J. Yunnan Nationalities Univ., Natural Sci. Ed.*, vol. 29, no. 1, pp. 70–77, 2020.

[13] W. Z. Ning, "Research on noise reduction function of compressed sensing in ship-radiated noise," *Ship Sci. Technol.*, vol. 39, no. 10, pp. 112–116, 2017.

[14] N. E. Huang, Z. Shen, S. R. Long, M. C. Wu, H. H. Shih, Q. Zheng, N.-C. Yen, C. C. Tung, and H. H. Liu, "The empirical mode decomposition and the Hilbert spectrum for nonlinear and non-stationary time series analysis," *Proc. Roy. Soc. London A, Math., Phys. Eng. Sci.*, vol. 454, no. 1971, pp. 903–995, Mar. 1998.

[15] Z. Wu and N. E. Huang, "Ensemble empirical mode decomposition: A noise-assisted data analysis method," *Adv. Adapt. Data Anal.*, vol. 1, no. 1, pp. 1–41, Jan. 2009.

[16] M. E. Torres, M. A. Colominas, G. Schlotthauer, and P. Flandrin, "A complete ensemble empirical mode decomposition with adaptive noise," in *Proc. IEEE Int. Conf. Acoust., Speech Signal Process. (ICASSP)*, May 2011, Art. no. 5947265.

[17] R. Deering and J. F. Kaiser, "The use of a masking signal to improve empirical mode decomposition," in *Proc. IEEE Int. Conf. Acoust., Speech Signal*, Mar. 2005, pp. 485–488.

[18] Y.-H. Wang, K. Hu, and M.-T. Lo, "Uniform phase empirical mode decomposition: An optimal hybridization of masking signal and ensemble approaches," *IEEE Access*, vol. 6, pp. 34819–34833, 2018.

[19] V. Veeraiyan, R. Velayutham, and M. M. Philip, "Frequency domain based approach for denoising of underwater acoustic signal using EMD," *J. Intell. Syst.*, vol. 22, no. 1, pp. 67–80, Mar. 2013.

[20] Y. Hong, L. Ya-an, and L. Guo-Hui, "Noise reduction method of ship radiated noise with ensemble empirical mode decomposition of adaptive noise," *Noise Control Eng. J.*, vol. 64, no. 2, pp. 230–242, Mar. 2016.

[21] Y. Li, Y. Li, X. Chen, J. Yu, H. Yang, and L. Wang, "A new underwater acoustic signal denoising technique based on CEEMDAN, mutual information, permutation entropy, and wavelet threshold denoising," *Entropy*, vol. 20, no. 8, p. 563, Jul. 2018.

[22] G. Li, Z. Yang, and H. Yang, "Noise reduction method of underwater acoustic signals based on uniform phase empirical mode decomposition, amplitude-aware permutation entropy, and Pearson correlation coefficient," *Entropy*, vol. 20, no. 12, p. 918, Nov. 2018.

[23] K. Dragomiretskiy and D. Zosso, "Variational mode decomposition," *IEEE Trans. Signal Process.*, vol. 62, no. 3, pp. 531–544, Feb. 2014.

[24] Y. Li, X. Chen, J. Yu, and X. Yang, "A fusion frequency feature extraction method for underwater acoustic signal based on variational mode decomposition, duffing chaotic oscillator and a kind of permutation entropy," *Electronics*, vol. 8, no. 1, p. 61, Jan. 2019.

[25] Y. Li, Y. Li, X. Chen, and J. Yu, "A novel feature extraction method for ship-radiated noise based on variational mode decomposition and multi-scale permutation entropy," *Entropy*, vol. 19, no. 7, p. 342, Jul. 2017.

[26] Q. Huang, L. Xie, G. Yin, M. Ran, X. Liu, and J. Zheng, "Acoustic signal analysis for detecting defects inside an arc magnet using a combination of variational mode decomposition and beetle antennae search," *ISA Trans.*, vol. 102, pp. 347–364, Jul. 2020.

[27] M. Liu, Y. T. Zhang, Z. N. Li, and H. B. Fan, "Enging fault diagnosis based on independent variational mode decomposition and improved kernel extreme learning machine," *J. Vib., Meas. Diagnosis*, vol. 39, no. 4, pp. 875–883, 2019.

[28] C. Zhang, Y. B. Zhang, C. X. Hu, Z. B. Liu, L. Y. Cheng, and Y. Zhou, "A novel intelligent fault diagnosis method based on variational mode decomposition and ensemble deep belief network," *IEEE Access*, vol. 8, pp. 36293–36312, 2020.

[29] Y. G. Zhang, Y. Zhao, and S. Gao, "A novel hybrid model for wind speed prediction based on VMD and neural network considering atmospheric uncertainties," *IEEE Access*, vol. 7, pp. 60322–60332, 2019.

[30] Y. Zhang, P. Han, D. F. Wang, and S. R. Wang, "Short-term prediction of wind speed for wind farm based on variational model decomposition and LSSVM model," *Acta Energine Solaris Sinica*, vol. 39, no. 1, pp. 194–202, 2018.

[31] H. Yang, L. P. Gao, and G. H. Li, "Underwater acoustic signal prediction based on correlation variational modal decomposition and error compensation," *IEEE Access*, vol. 8, pp. 103941–103955, 2020.

[32] H. Yang, L. P. Gao, and G. H. Li, "Underwater acoustic signal prediction based on MVMD and optimized kernel extreme learning machine," *Complexity*, vol. 2020, Apr. 2020, Art. no. 6947059.

[33] C. J. Zhou, J. Ma, J. Wu, and X. Y. Yuan, "An adaptive VMD method based on improved GOA to extract early fault feature of rolling bearings," *Int. J. Innov. Comput., Inf. Control*, vol. 15, no. 4, pp. 1485–1505, 2019.

[34] S. Pincus, "Approximate entropy (ApEn) as a complexity measure," *Chaos, Interdiscipl. J. Nonlinear Sci.*, vol. 5, no. 1, pp. 110–117, Mar. 1995.

[35] J. S. Richman and M. J. Randall, "Physiological time-series analysis using approximate entropy and sample entropy," *Amer. J. Physiol.-Heart Circulatory Physiol.*, vol. 278, no. 6, pp. 2039–2049, 2000.

[36] W. Chen, Z. Wang, H. Xie, and W. Yu, "Characterization of surface EMG signal based on fuzzy entropy," *IEEE Trans. Neural Syst. Rehabil. Eng.*, vol. 15, no. 2, pp. 266–272, Jun. 2007.

[37] C. Bandt and B. Pompe, "Permutation entropy: A natural complexity measure for time series," *Phys. Rev. Lett.*, vol. 88, no. 17, Apr. 2002, Art. no. 174102.

[38] M. Rostaghi and H. Azami, "Dispersion entropy: A measure for time-series analysis," *IEEE Signal Process. Lett.*, vol. 23, no. 5, pp. 610–614, May 2016.

[39] H. Azami, E. Kinney-lang, A. Ebied, A. Fernandez, and J. Escudero, "Multiscale dispersion entropy for the regional analysis of resting-state magnetoencephalogram complexity in Alzheimer's disease," in *Proc. 39th Annu. Int. Conf. IEEE Eng. Med. Biol. Soc. (EMBC)*, Jul. 2017, Art. no. 8037533.

[40] H. Azami, A. Fernández, and J. Escudero, "Multivariate multiscale dispersion entropy of biomedical times series," *Entropy*, vol. 21, no. 9, p. 913, Sep. 2019.

[41] Z. Chen, Y. Li, R. Cao, W. Ali, J. Yu, and H. Liang, "A new feature extraction method for ship-radiated noise based on improved CEEMDAN, normalized mutual information and multiscale improved permutation entropy," *Entropy*, vol. 21, no. 6, p. 624, Jun. 2019.

[42] Y. Li, Y. Li, X. Chen, and J. Yu, "Research on ship-radiated noise denoising using secondary variational mode decomposition and correlation coefficient," *Sensors*, vol. 18, no. 2, p. 48, Dec. 2017.

[43] G. Li, Z. Yang, and H. Yang, "A denoising method of ship radiated noise signal based on modified CEEMDAN, dispersion entropy, and interval thresholding," *Electronics*, vol. 8, no. 6, p. 597, May 2019.

[44] G. Li, Q. Guan, and H. Yang, "Noise reduction method of underwater acoustic signals based on CEEMDAN, Effort-To-Compress complexity, refined composite multiscale dispersion entropy and wavelet threshold denoising," *Entropy*, vol. 21, no. 1, p. 11, Dec. 2018.

[45] Y.-X. Li and L. Wang, "A novel noise reduction technique for underwater acoustic signals based on complete ensemble empirical mode decomposition with adaptive noise, minimum mean square variance criterion and least mean square adaptive filter," *Defence Technol.*, vol. 16, no. 3, pp. 543–554, Jun. 2020.

[46] M. Li, D. M. Guo, J. F. Quan, and X. Y. Zheng, "Improved half-soft threshold denoising based on lifting wavelet," *J. Detection Control*, vol. 31, no. 4, pp. 54–57, 2009.

[47] Z. H. Zhao, S. P. Yang, and Y. J. Shen, "Improved EMD based de-noising method," *J. Vib. Shock*, vol. 28, no. 12, pp. 35–37, 2009.

[48] X. L. Wei, R. L. Lin, S. Y. Liu, and Q. C. Yang, "A de-noising method for chaotic signals based on improved EEMD," *J. Vib. Shock*, vol. 36, no. 17, pp. 35–41, 20, 2017.

[49] G. Li, W. Chang, and H. Yang, "A novel combined prediction model for monthly mean precipitation with error correction strategy," *IEEE Access*, vol. 8, pp. 141432–141445, 2020, doi: 10.1109/ACCESS.2020.3013354.

[50] J. Chen, Z. Zhu, and X. Zhang, "Feature cognitive model combined by an improved variational mode and singular value decomposition for fault signals," *Cognit. Comput. Syst.*, vol. 2, no. 2, pp. 66–71, Jun. 2020.
[51] D. Luo, T. Wu, M. Li, B. Yi, and H. Zuo, "Application of VMD and Hilbert transform algorithms on detection of the ripple components of the DC signal," *Energies*, vol. 13, no. 4, p. 935, Feb. 2020.
[52] W. Gao, L. Hu, and P. Zhang, "Class-specific mutual information variation for feature selection," *Pattern Recognit.*, vol. 79, pp. 328–339, Jul. 2018.
[53] M. U. Ahmed and D. P. Mandic, "Multivariate multiscale entropy: A tool for complexity analysis of multichannel data," *Phys. Rev. E, Stat. Phys. Plasmas Fluids Relat. Interdiscip. Top.*, vol. 84, no. 6, Dec. 2011, Art. no. 061918.
[54] F. Samann and T. Schanze, "An efficient ECG denoising method using discrete wavelet with Savitzky-Golay filter," *Current Direction Biomed. Eng.*, vol. 5, no. 1, pp. 385–388, 2019.
[55] H. L. Kennedy, "Improving the frequency response of Savitzky-Golay filters via colored-noise models," *Digit. Signal Process.*, vol. 102, Jul. 2020, Art. no. 102743.
[56] H. Kaneko, T. Matsumoto, S. Ootakara, and K. Funatsu, "Practical use of Savitzky-Golay filtering-based ensemble online SVR," *IFAC-PapersOnLine*, vol. 49, no. 7, pp. 371–376, 2016.
[57] F. B. Zhou, C. G. Li, and H. Q. Zhu, "Research on threshold improved denoising algorithm based on lifting wavelet transform in UV-Vis spectrum," *Spectrosc. Spectral Anal.*, vol. 38, no. 2, pp. 506–510, 2018.
[58] Y. Li, B. K. Via, and Y. Li, "Lifting wavelet transform for vis-NIR spectral data optimization to predict wood density," *Spectrochimica Acta A, Mol. Biomolecular Spectrosc.*, vol. 240, Oct. 2020, Art. no. 118566.
[59] X. Xu, "Single pulse threshold detection method with lifting wavelet denoising based on modified particle swarm optimization," *Infr. Phys. Technol.*, vol. 88, pp. 174–183, Jan. 2018.
[60] X. J. Wu, "Improved wavelet threshold based on lifting wavelet in application of signal de-noising," *Lasernal*, vol. 35, no. 8, pp. 15–18, 2014.
[61] Z. Liu, Y. G. Zhou, S. Y. Zou, and X. Y. Zhang, "Study on lifting wavelet improved threshold de-noising method for acoustic emission signal of hydraulic turbine cavitation," *Water Power*, vol. 45, no. 8, pp. 85–89, 98, 2019.
[62] M. Sadeghi, F. Behnia, and R. Amiri, "Window selection of the Savitzky–Golay filters for signal recovery from noisy measurements," *IEEE Trans. Instrum. Meas.*, vol. 69, no. 8, pp. 5418–5427, Aug. 2020.
[63] T. Chai and R. R. Draxler, "Root mean square error (RMSE) or mean absolute error (MAE)?—Arguments against avoiding RMSE in the literature," *Geosci. Model Develop.*, vol. 7, no. 1, pp. 1525–1534, 2014.
[64] Y. X. Xu, W. P. Yang, and L. Y. Ren, "Application of fractal theory to fault diagnosis of vehicle engine," *J. Vib., Meas. Diagnosis*, vol. 21, no. 4, pp. 275–280, 296, 2001.
[65] Z. M. Li, X. T. Gou, and W. D. Jing, "Correlation dimension of microseismic signal," *J. Detection Control*, vol. 30, no. 4, pp. 76–80, 2008.
[66] N. Li and Y. J. Fang, "Fault signal analysis of mechanical system based on correlation dimension," *J. Vib. Shock*, vol. 26, no. 4, pp. 136–139, 2007.
[67] D. M. Anderson and J. F. Gillooly, "Allometric scaling of Lyapunov exponents in chaotic populations," *Population Ecol.*, vol. 62, no. 3, pp. 364–369, Jul. 2020.
[68] Z. Q. Ma, Y. C. Li, Z. Liu, and C. J. Gu, "Rolling bearings' fault feature extraction based on variational mode decomposition and Teager energy operator," *J. Vib. Shock*, vol. 35, no. 13, pp. 134–139, 2016.
[69] D. Santos-Domínguez, S. Torres-Guijarro, A. Cardenal-López, and A. Pena-Gimenez, "ShipsEar: An underwater vessel noise database," *Appl. Acoust.*, vol. 113, pp. 64–69, Dec. 2016.

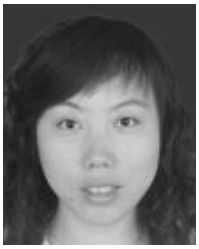

HONG YANG received the bachelor's and master's degrees in mechanical and electronics engineering from the University of Electronic Science and Technology of China, Chengdu, China, in 2003 and 2006, respectively, and the Ph.D. degree in acoustics from Northwestern Polytechnical University, Xi'an, China, in 2015. She is an Associate Professor with the School of Electronics Engineering, Xi'an University of Posts and Telecommunications, Xi'an. Her research interests include underwater acoustic signal processing and chaotic signal processing.

LULU LI received the bachelor's degree in electronic information science and technology from Xinzhou Teachers University, Xinzhou, China, in 2019. She is currently pursuing the master's degree in electronics and communication engineering with the Xi'an University of Posts and Telecommunications, Xi'an, China. Her research interests include underwater acoustic signal noise reduction and chaotic signal processing.

GUOHUI LI received the bachelor's degree in electronic information engineering from the Chongqing University of Technology, Chongqing, China, in 2001, the master's degree in circuits and systems from the University of Electronic Science and Technology of China, Chengdu, China, in 2004, and the Ph.D. degree in acoustics from Northwestern Polytechnical University, Xi'an, China, in 2015. He is an Associate Professor with the School of Electronics Engineering, Xi'an University of Posts and Telecommunications, Xi'an, China. His research interests include underwater acoustic signal processing and chaotic signal processing.